JOURNAL OF THE CANADIAN SOCIETY OF EXPLORATION GEOPHYSICISTS
VOL. 22, NO. 1 (DEC. 1986), P. 7-16

SUITABLE ENVIRONMENTS FOR INVERSION TECHNIQUES: A MODEL STUDY[1]

SUDHIR JAIN[2]

ABSTRACT

In order to determine the applicability of inversion to various lithological environments, a set of normal incidence synthetic traces was generated by using an 8/12-55/65 Hz zero phase wavelet for four synthetic logs from the following environments: 1) Gething sands in the deep basin of Alberta located close to a coal bed. 2) A glauconitic sand in southern Alberta. 3) Carbonate porosity near the top of carbonates in northern Alberta. 4) Granite Wash sand deposits in northern Alberta.

In each case two sets of synthetics were generated by altering the velocity contrast for a thin layer and by altering the thickness for a reasonable velocity contrast. In all models, very thin layers cause changes in velocity of a zone of approximately 10 ms (20 to 30 m) duration. This change is related in magnitude to both the thickness of the zone and the magnitude of the contrast. From these thin-layer models, it does not seem possible to estimate both the thickness and the velocity contrast of the zone of interest but the presence of a thin layer can be predicted. Thus, with current data it is possible to identify the thin zones of porous sandstones or carbonates and get a qualitative idea of their economic value. However, their thickness and porosity cannot be estimated on the inversion section.

The following conclusions are derived for specific cases:

1. Coal beds do not interfere with Gething sand on the inversion sections. These sands can be identified distinctly when the total thickness of the sand zone is at least 8 m for a velocity contrast of 850 m/s or the velocity contrast is at least 600 m/s for 12-m-thick sand.

2. A 4-m-thick Glauconitic sand with a velocity contrast of 450 m/s causes an identifiable velocity difference. An 8-m-thick sand zone can be identified when the velocity contrast is only 300 m/s.

3. Carbonate porosity can be identified when the velocity contrast is 4% for an 18-m-thick zone. A velocity contrast of 5% can be identified when this zone is 12 m thick.

4. Granite Wash can be identified when it is less than 5 m thick. However, small changes in Precambrian structure (up to 20 m) cannot be identified.

In conclusion, the synthetic models with a wavelet representing the bandwidth of most seismic data show that the inversion technique can identify relatively thin productive zones in a wide variety of geological environments. Some examples are shown for similar, but not identical, situations in real data.

INTRODUCTION

The interval velocity of the layered medium traversed by seismic waves can be computed from the surface response of a source from normal moveout, lateral displacement of reflection points, and the amplitude of the reflections. The first two measurements provide variations in velocities over large intervals of hundreds of metres, while the changes over small intervals of up to a few metres can be estimated from amplitudes. The combination usually provides reasonably accurate estimates of the interval velocities. Such estimates have come into increasing use in hydrocarbon exploration over recent years. The available techniques of estimating interval velocities — generally called inversion — show marked differences in underlying concepts, computer algorithms and presentation (Delas *et al.*, 1970; Lindseth, 1979; Oldenburg, 1983; Cooke and Schneider, 1983). This paper discusses the results obtained by one inversion technique (Jain and Wren, 1977) in four synthetic stratigraphic situations, and makes some general conclusions regarding resolution limits in these situations. It must be emphasized that the conclusions derived here may apply to other techniques in a general way but not in specific terms. It may also be noted that an inversion section is the estimate of impedance distribution. Relating this to lithology is still ambiguous, particularly when thin beds are involved.

Carefully processed and deconvolved (noise-free) seismic data are equivalent to the convolution of a band-limited wavelet with the reflectivity index series of the traversed medium. The resolution of the reflectivity index series computed from sonic logs depends only on the sample interval of the data. However, the resolution of seismic traces is a function of bandwidth and phase-spectrum of the wavelet. Bandwidth determines the minimum separation in reflectivity indices that can be observed on a trace (thinner beds are smoothed or filtered out) and the phase determines which reflectivity indices are tuned in or tuned out. The tuning effect

[1]Contribution to a Panel Discussion on Inversion, C.S.E.G. Annual Meeting, May 15, 1986

[2]Commonwealth Geophysical Development Company, Ltd., #1701, 505-3 Street S.W., Calgary, Alberta T2P 3E6

The kindness of oil companies in releasing the data for this paper is appreciated. The author has benefitted from his many discussions on inversion with Mr. W.W. Soukoreff of Petro-Canada I.A.C.

can be minimized by computing the wavelet and reducing it to a spike. On the other hand, very thin beds are filtered by the wavelet to amplitudes below the dynamic range of the data, and these cannot be recovered. The amplitude spectrum of the wavelet and the magnitude of the reflectivity indices determine the minimum detectable thickness of these thin beds. Slightly thicker beds of reasonable acoustic impedance contrast cause amplitude or character differences that are below the display range but within the dynamic range of the data. In favourable circumstances, these beds can be identified after inversion. It is the purpose of this paper to estimate the thickness and velocity contrast of such beds in some situations of practical interest.

Synthetic Models and Analytical Procedure

Four sonic logs were chosen from Alberta, each representing a stratigraphic environment of exploration interest. Sonic logs were integrated at a 2-ms (two-way) interval and the zone of interest was modifed in the integrated sonic in two ways:

1. The velocity in the critical zone was changed within the expected limits at regular intervals.

2. The thickness of the critical zone was changed in small increments from zero to a reasonably thick section.

The modified integrated sonic velocities were converted to acoustic impedance and reflectivity series by assuming that the empirical density/velocity relationship given by Gardner *et al.* (1974) is applicable. A zero-phase filter of trapezoidal passband 8/12-55/65 Hz was applied to the reflectivity indices to obtain synthetic traces. The impulse response of this filter is shown in Figure 1. In the author's experience, this frequency band is representative of much of the data collected in Alberta over the last few years. No noise of any kind was added, nor were any corrections made for absorption, because the influence of noise was not the purpose of this study. Therefore, the results obtained here are applicable only to relatively noise-free data which, fortunately, often occur. In other cases, enhancement techniques are available to improve data to an acceptable level (Jain, 1985). It may be noted that the level of signal/noise ratio required for adequate inversion is a function of the type of noise rather than its magnitude. Weak multiples are generally more misleading than a significant level of random noise.

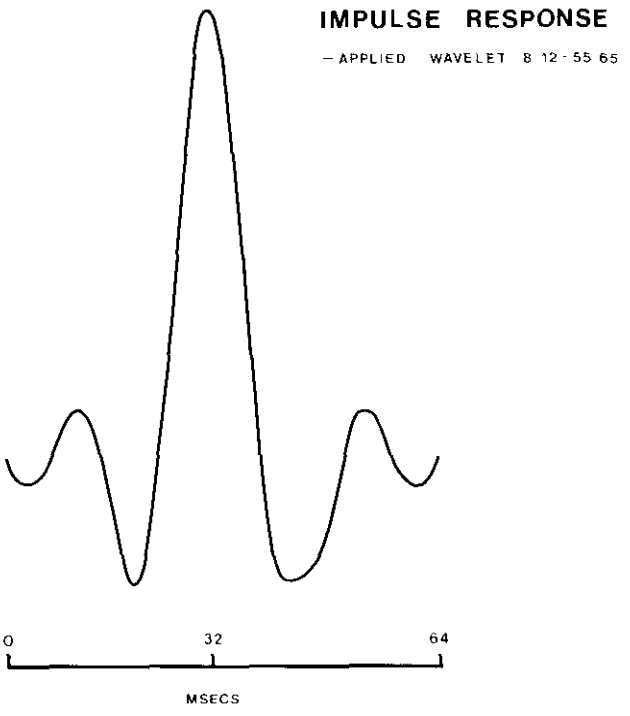

Fig. 1. Impulse response of applied wavelet.

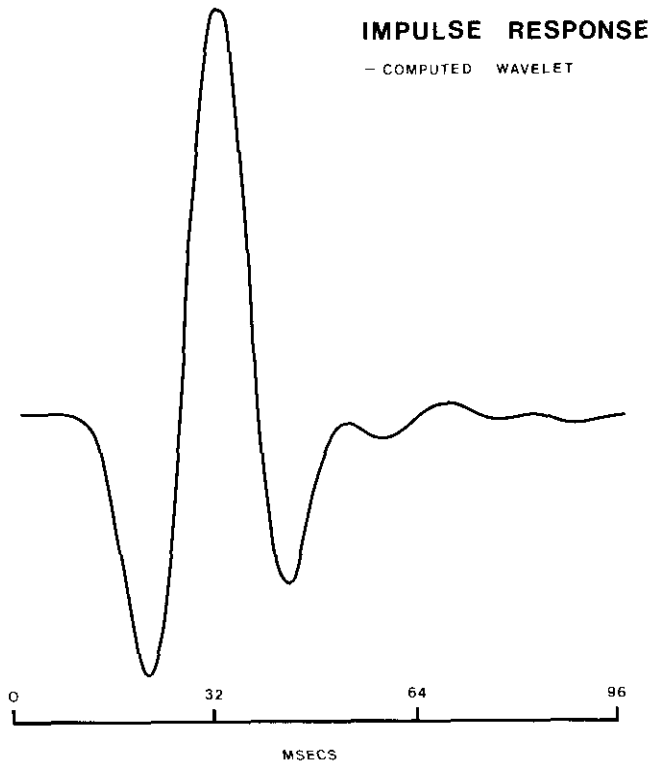

Fig. 2. Impulse response of computed wavelet.

Inversion Technique

Jain and Wren (1977) discussed various aspects of inversion including the significance of the phase of the propagating wavelet and the signal/noise ratio requirements. The inversion technique outlined in that paper was used in this study. An approximation of the propagating wavelet was computed for each trace (Fig. 2). The operators were designed to reduce wavelets to spikes and applied to the respective traces. Figure 3 shows the computed wavelets for a group of synthetic traces and the results of convolution with the designed operators. The resulting reflectivity index traces were used to compute interval velocities (Gardner *et al.*, 1974).

A small difference in phase can be noted between the applied and computed wavelets (Figs. 1, 2). The inversion results are influenced by this error in two ways:

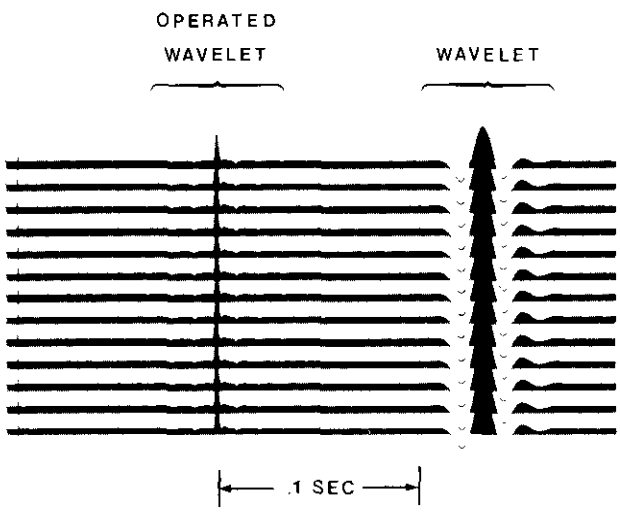

Fig. 3. Computed wavelets for a group of synthetic traces and results of convolution with the designed operators.

1. The error causes a small time-shift between inverted traces and sonic logs. For the reader's convenience, the displays have been adjusted for this time-shift.

2. This difference in wavelets introduces some inaccuracies in the vicinity of large velocity contrasts. It is important to compare inversion velocities with available sonic logs to estimate the significance of these inaccuracies.

Offset Amplitude - Model

It has been stated (Wren, 1984) that because of the appreciable change in reflectivities with offset distance computed according to equations given by Zoeppritz (Telford *et al.*, 1976) the stacking process may not be valid and inversion of stacked data may be misleading. This is generally true when spread distance and depth to reflector are such that the angle of incidence is greater than 30°. In such cases one needs to adjust sonic velocities for the effects of offset, and compute a 'stacked sonic log'. In most cases, however, this measure is not necessary. Figure 4 shows the reflectivity index traces before and after application of the wavelet shown in Figure 1 for spread distances ranging from 0 to 1650 m and for depths of 1700 to 2200 m. 'Stacked' reflectivities and velocities computed from these reflectivities are also shown for comparison. While the amplitudes show certain decay with increasing offset, the stacked trace and velocities correspond very closely to their zero-offset versions after a constant scale adjustment. If equalization were to be applied, as is generally done in processing, the scale difference present in Figure 4 would become miniscule. This example confirms the general validity of stacking procedures when relative variations are being investigated, while not discouraging amplitude vs offset studies when absolute variations are desired and can be reliably computed from data.

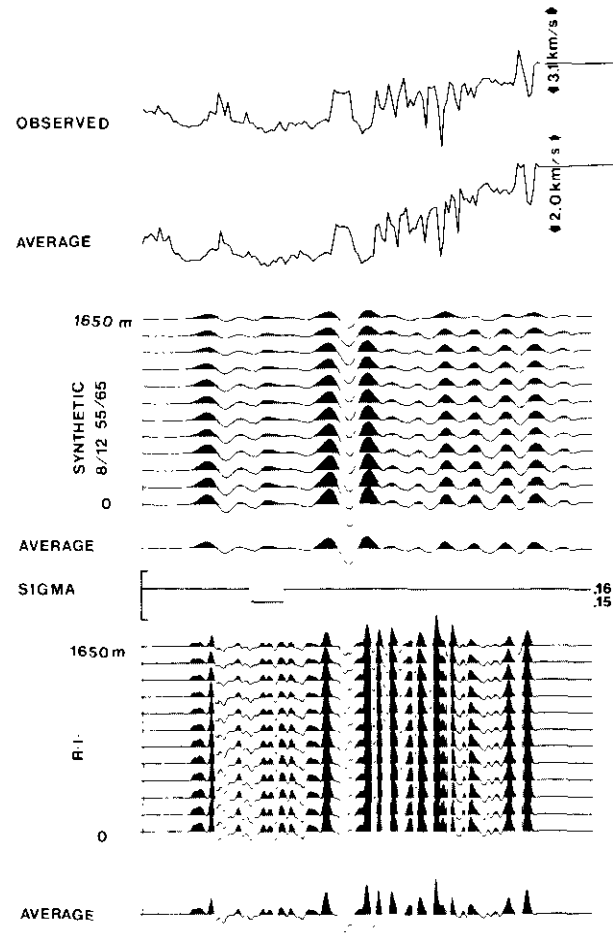

Fig. 4. Offset synthetics vs average synthetic; heavy lines are 50 ms apart.

Description of Models

The following situations were investigated by modelling:

1. Gething sand deposit in the deep basin in central Alberta, near a coal bed (Well 10-34-T69 R5 W6M).

2. Glauconitic sand deposit in southern and central Alberta (Well 14-18-T42 R25 W4M).

3. Carbonate porosity near the top of carbonates in northern Alberta (Well 2-4-T63 R12 W5M).

4. Granite Wash deposits in northern Alberta (Well 4-2-T83 R9 W5M).

While any number of other situations can be visualized, many of these can be considered slight deviations of one of the above. Each situation is discussed individually. In each case the altered integrated sonic logs are shown on the top, corresponding synthetic traces at the bottom, and the traces after inversion in the middle. The figures show 200 ms of data around the zone of interest. The depths are given in the captions and the text. Real data examples are shown with considerable vertical exaggeration. These are given as general illustrations and do not necessarily correspond to the sonic logs in the modelled situations. The shade or colour interval in the inversion plots is 100 or 200 m/s and is given on each figure.

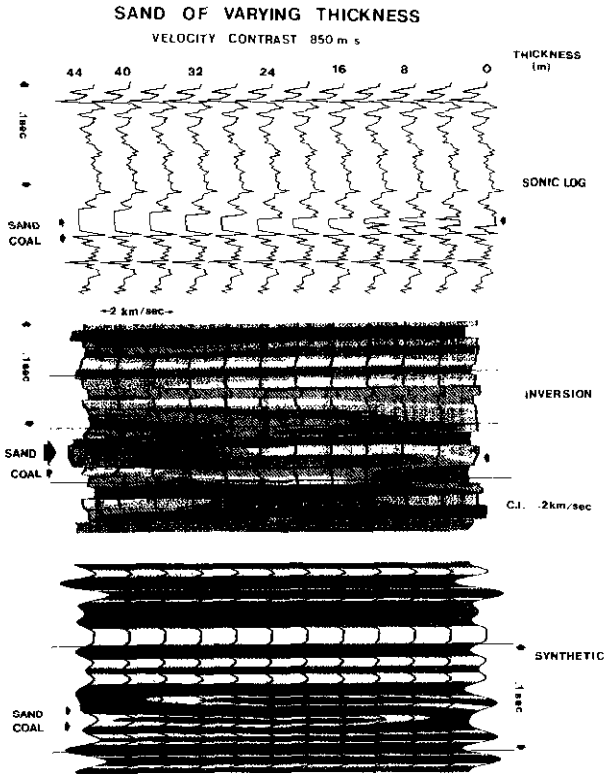

Fig. 5. Sand of varying thickness in vicinity of coal bed. Sand and coal beds are marked with arrows. Note that sand zone can be identified when it is 8 m thick. Depth section shown is for 1560-2000 m from surface.

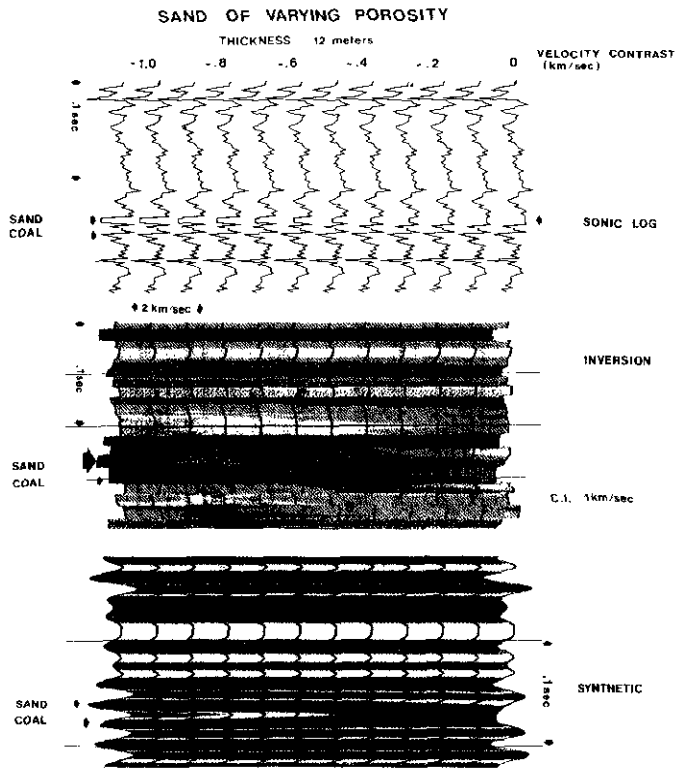

Fig. 6. Sand of varying porosity in vicinity of coal bed. Sand and coal are marked by arrows. Velocity contrast range corresponds roughly to porosity increase from 10% to 35%. Note that sand can be identified when velocity contrast is 500 m/s.

Results and Discussion

Sand Deposit in Deep Basin

In Figures 5 and 6 Gething (Lower Cretaceous) sand is located at 1.064 s. A prominent coal marker is visible at 1.080 s. In Figure 5 the sand has a velocity 850 m/s less than the surrounding shales, increasing in thickness from 0-44 m at 4-m intervals. At 4 m the sand is barely noticed even on noise-free data, but at 8 m a clear low exceeding 100 m/s is noted. As the sand thickness increases, the magnitude of contrast increases as well, but the noted thickness remains at 8-10 ms until the sand thickens so much that the upper high-velocity shale becomes too thin to be observed. This and the following models show that thin beds are averaged over the resolution limit set by the frequency ranges of seismic data. For the synthetic traces in this study, this limit is observed to be 8 to 10 ms (20-25 m). Thinner beds are observed indirectly, because they influence the average over this range which shows some of the velocity contrast of the thin bed. As the thickness of the thin bed increases (36 m in Fig. 5) the observed velocity contrast approaches the real velocity contrast. Also note that sand bed variations occur 10 ms above the coal bed and are distinctive. While synthetics show amplitude buildup at 16-32 m thickness for a wide zone relative to sand thickness, followed by rapid decay as the thickness increases, inversion is unique for all thickness levels and there is little chance of confusion with the coal bed.

Figure 6 shows the same sonic except that, in this case, the sand thickness is constant at 12 m and the velocity contrast increases from 200 m/s to 1400 m/s. When expected matrix and water velocities are substituted in the equation given by Kuster and Toksoz (1974), they correspond to porosities in sand of 10-35%. Again, the observed thickness of the sand zone is 10 ms (20 m) which becomes quite distinct when the velocity contrast is 600 m/s. The observed contrast increases with increasing contrast in the sonic but never approaches the actual value, presumably because the bed is too thin to be observed accurately by the assumed propagating wavelet. Again, the sand and coal beds are clearly separated on the inversion traces.

Figure 7 shows a real data example where productive Halfway sand — a deeper sand than that in the model — is clearly indicated by a low-velocity zone (green) in the right half of the section. More-porous sand in the wells toward the east is marked by still lower velocity (yellow), and the absence of the Halfway sand environment is quite pronounced in the western half of the section (all blue, except for isolated green spots).

Glauconitic Sand Deposits

Figures 8, 9 and 10 show the section for the depths 1300-1670 m with Glauconitic sand at .964 s, 12 ms below a prominent coal marker. The assumed velocity contrast is 570 m/s and thickness increases from 0-20 m at

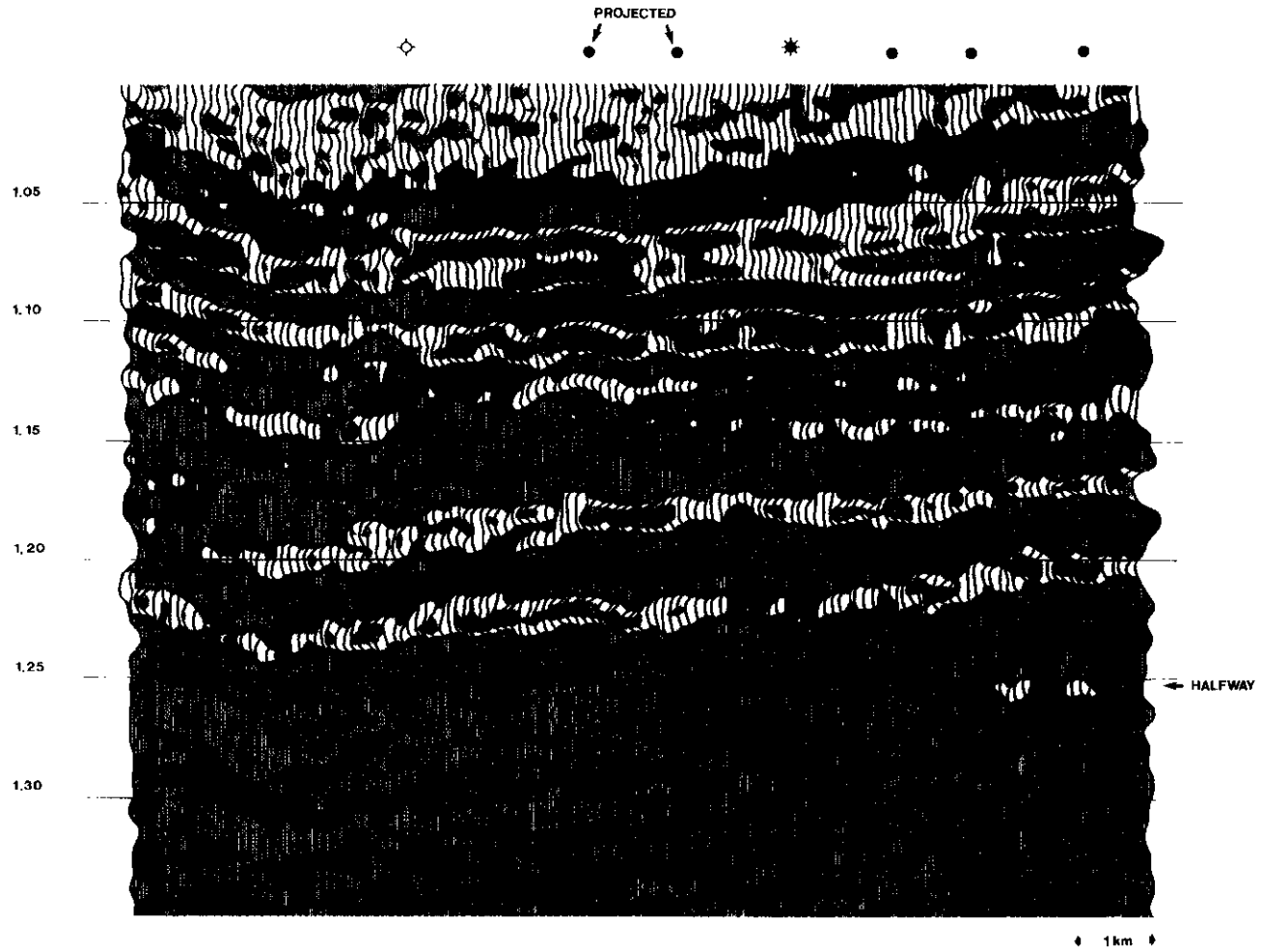

Fig. 7. Real data example of productive Halfway sand, indicated by prominent low (green and pale yellow) in the eastern half of the section; the sand dips westward from 1.25 s in the east.

4-m intervals (Fig. 8). The synthetic traces show some amplitude decay with increasing thickness. For the four traces on the right, inversion does not show the velocity low to correspond to the thin sand. Even the 12-m-thick sand is too thin to be identified by itself because the thinnest zone is some 20 m thick on the inversion traces. However, the presence of sand is noticeable in a reduction of velocity of this 20-m-thick zone even when the sand is only 4 m thick. When the sand is 16 and 20 m thick, the corresponding low-velocity zone becomes clear on the inversion but with less magnitude.

In Figure 9 the sand thickness is 4 m and the velocity contrast increases from 0 to 750 m/s at 150 m/s intervals. The reduction in the high-velocity zone becomes noticeable when the velocity contrast reaches 450 m/s. In Figure 10 the sand thickness is 8 m and this reduction can be noted when the contrast is 300 m/s. It appears from the models that the thinnest sand that can be observed is a function of velocity contrast (porosity, fluid content) as well as thickness. Relatively thin porous sand can be observed while impervious sand has to be thicker — for once the way we would like this to be!

Figure 11 shows a real data example where 3-m-thick porous Taber sand — a slightly different environment from that of the model — is identified by a lower velocity (red zone at .75 s) which is markedly absent where a dry well is located. Two other red zones to the right are probably connected to the drilled sand body.

Carbonate Porosity in Northern Alberta

Figures 12 and 13 show the sonic at the depth of 1550-1870 m with Slave Point carbonate top at 1.040 s. In Figure 12, the velocity of the carbonate marker is reduced by 5% over thicknesses increasing from 0 to 36 m in steps of 6 m. Synthetic traces do not show any significant differences, but in the inversion traces the velocity over the 30-m zone corresponding to limestone between two shales declines gradually such that the reduction becomes noticeable (100 m/s) when the thickness of the lower-velocity zone reaches 12 m and pronounced (200 m/s) at 30 m. However, the porosity zone is too thin for it to be seen in the inversion traces as a distinct step comparable to the sonic.

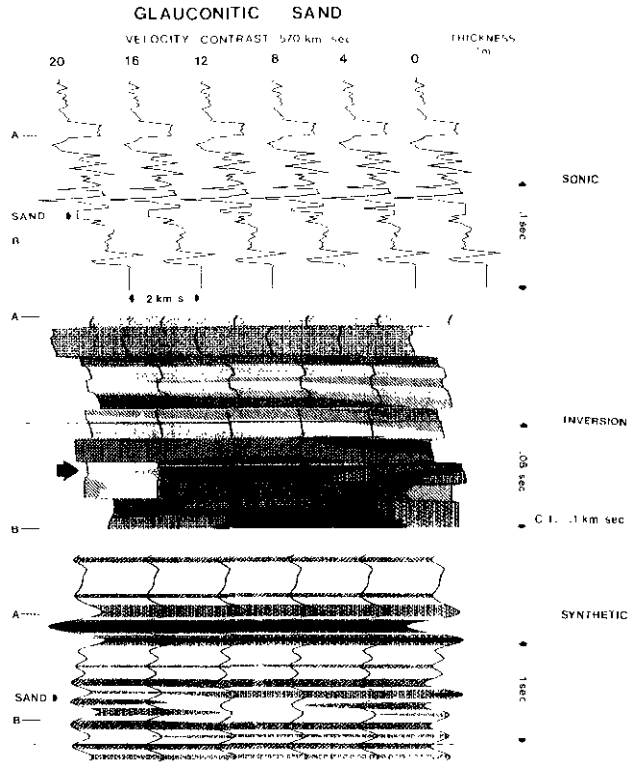

Fig. 8. Glauconitic sand with velocity contrast .570 kms/s with neighbouring shales and of varying thickness. The sand is detectable when 4 m thick.

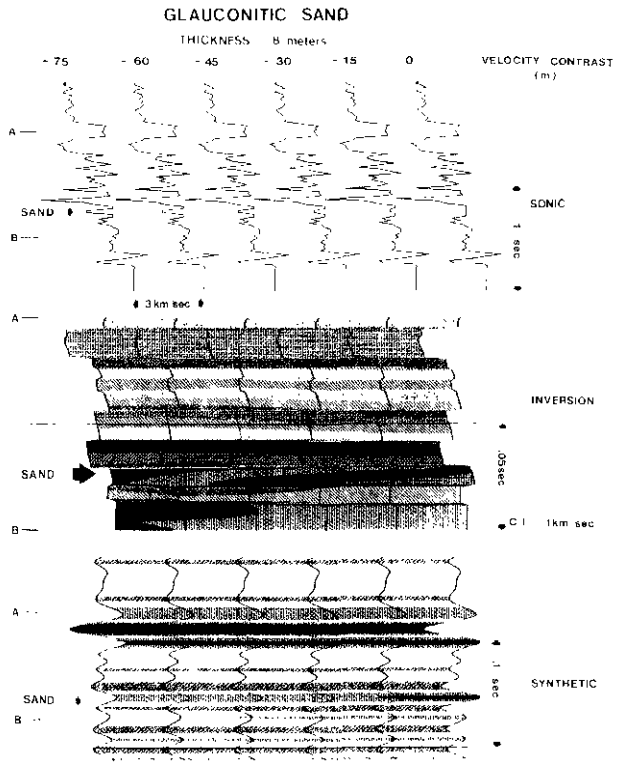

Fig. 10. Glauconitic sand of 8-m thickness and variable porosity. Velocity contrast after inversion in indicated zone between top and third inverted trace is 100 m/s, which suggests that 8-m-thick sand of velocity contrast with surrounding shales of 300 m/s could be detected.

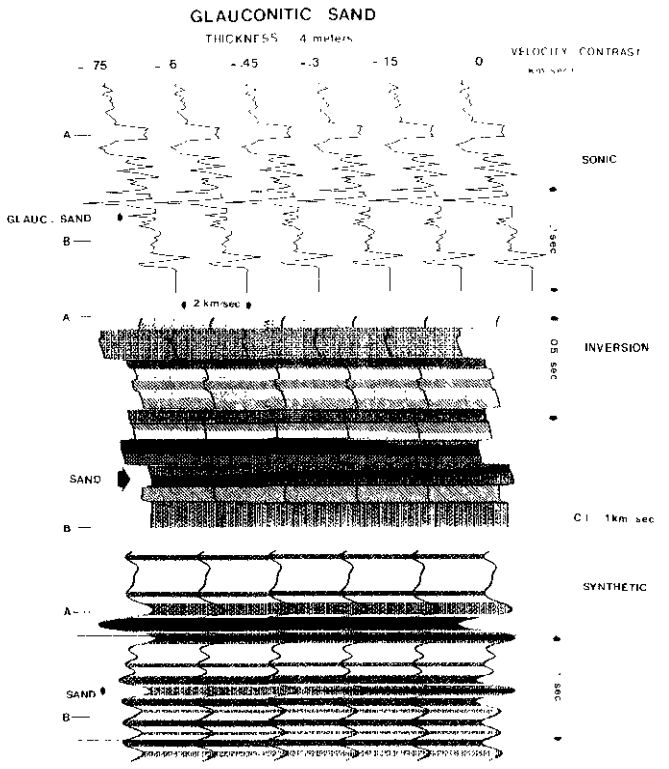

Fig. 9. Glauconitic sand of 4-m thickness and variable porosity. Velocity contrast after inversion in indicated zone between top and fourth inverted trace is 100 m/s, which suggests that 4-m-thick sand of velocity contrast with surrounding shales of 450 m/s should be detected.

In Figure 13 the thickness of the porosity zone is held constant and the velocity reduction is increased from 0 to 12% in steps of 2%. For water-filled limestone with largely fracture porosity (aspect ratio .05) these reductions correspond to a porosity increase from 4 to 12%. Again, the inversion traces show a general reduction in the carbonate zone rather than the notch that is prominent in sonics for highly porous carbonate. This reduction becomes noticeable (100 m/s) when the reduction is 4%, suggesting that 18-m-thick porosity zones can be detected if the porosity changes by only 2%. Just as in the case of thin sands, one cannot determine either thickness or velocity contrast but only an estimate of economic worth — a qualitative measure of thickness and porosity combined.

Figure 14 shows an example of a porous Keg River reef as seen on the inversion section. Figure 15 is an example of an inversion section as presented by Bower and Boyd (1986). This shows a buildup of Swan Hills reef between 1.55 and 1.57 s, and identification of porosity on the flanks of the reef (pink zones indicated by arrows).

Granite Wash in Northern Alberta

This model is generated a little differently from the other three models. Instead of providing the sand with a fixed velocity when the thickness is being changed, the sand (2830-2850 m, 1.674-1.684 s) was replaced by underlying Precambrian velocity, sample by sample (Fig. 16).

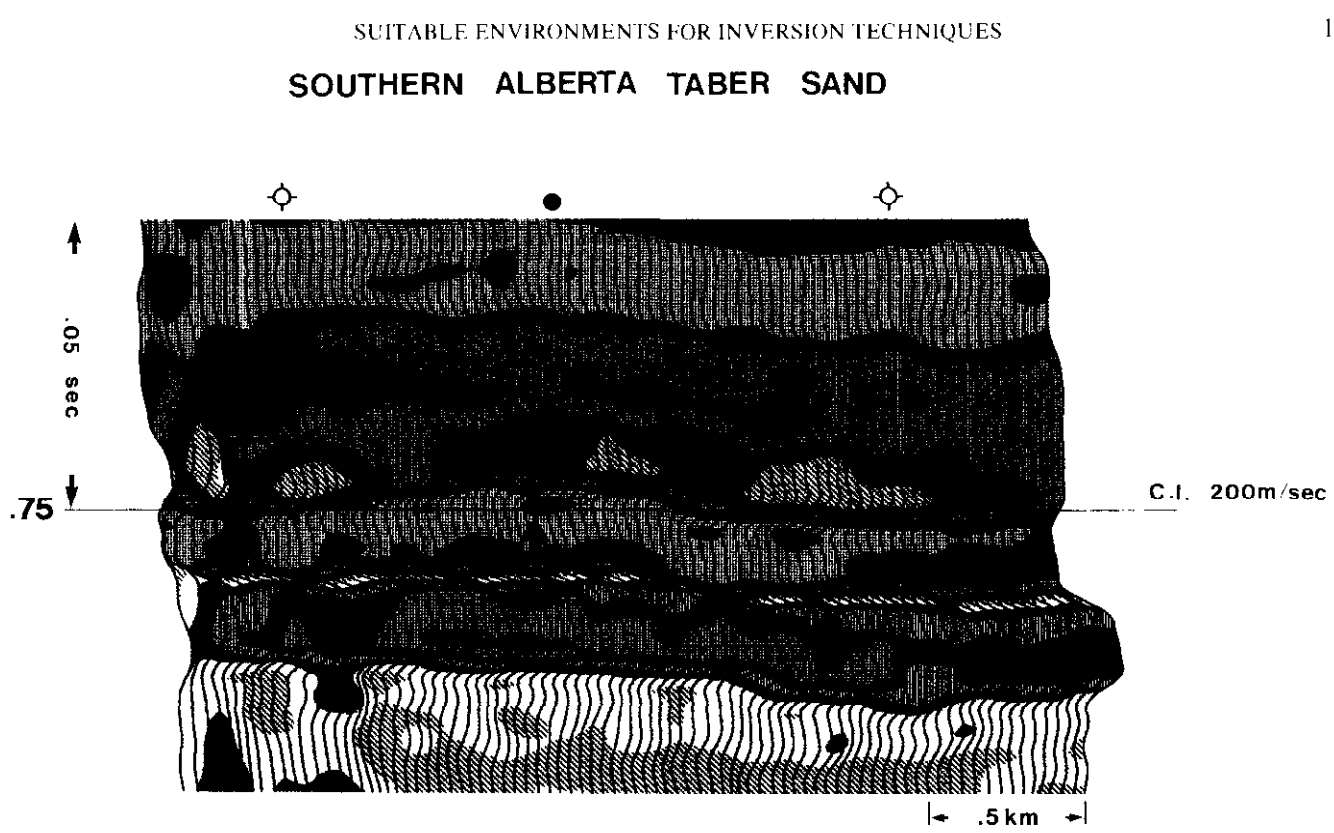

Fig. 11. Real data example where 3-m-thick porous oil-bearing sand is identified by lower velocity (red zones) at .75 s.

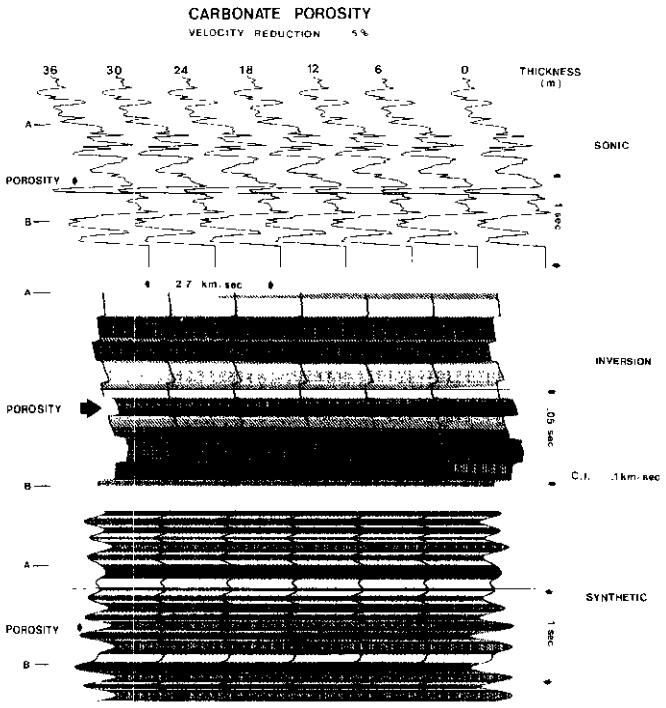

Fig. 12. Carbonate porosity near the top of Slave Point, velocity contrast constant at 5% and thickness increases from 0 to 36 m. Difference in inversion velocity approaches 100 m/s when thickness is 12 m.

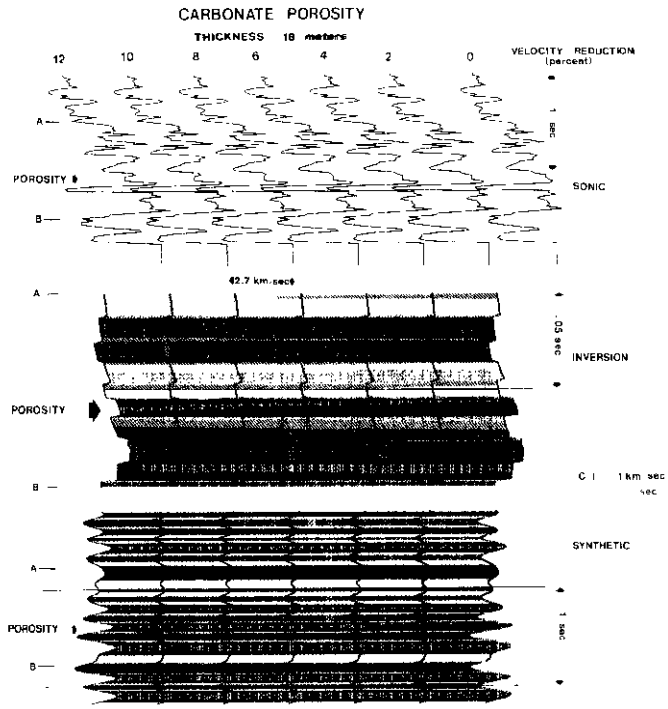

Fig. 13. Carbonate porosity near the top of Slave Point, thickness constant at 18 m and velocity contrast increases from 0 to 12%, which corresponds to porosity of 4 to 10% for water-filled carbonates with aspect ratio of .05 (Kuster and Toksoz, 1974). Difference in inversion velocity exceeds 100 m/s when contrast is 6%.

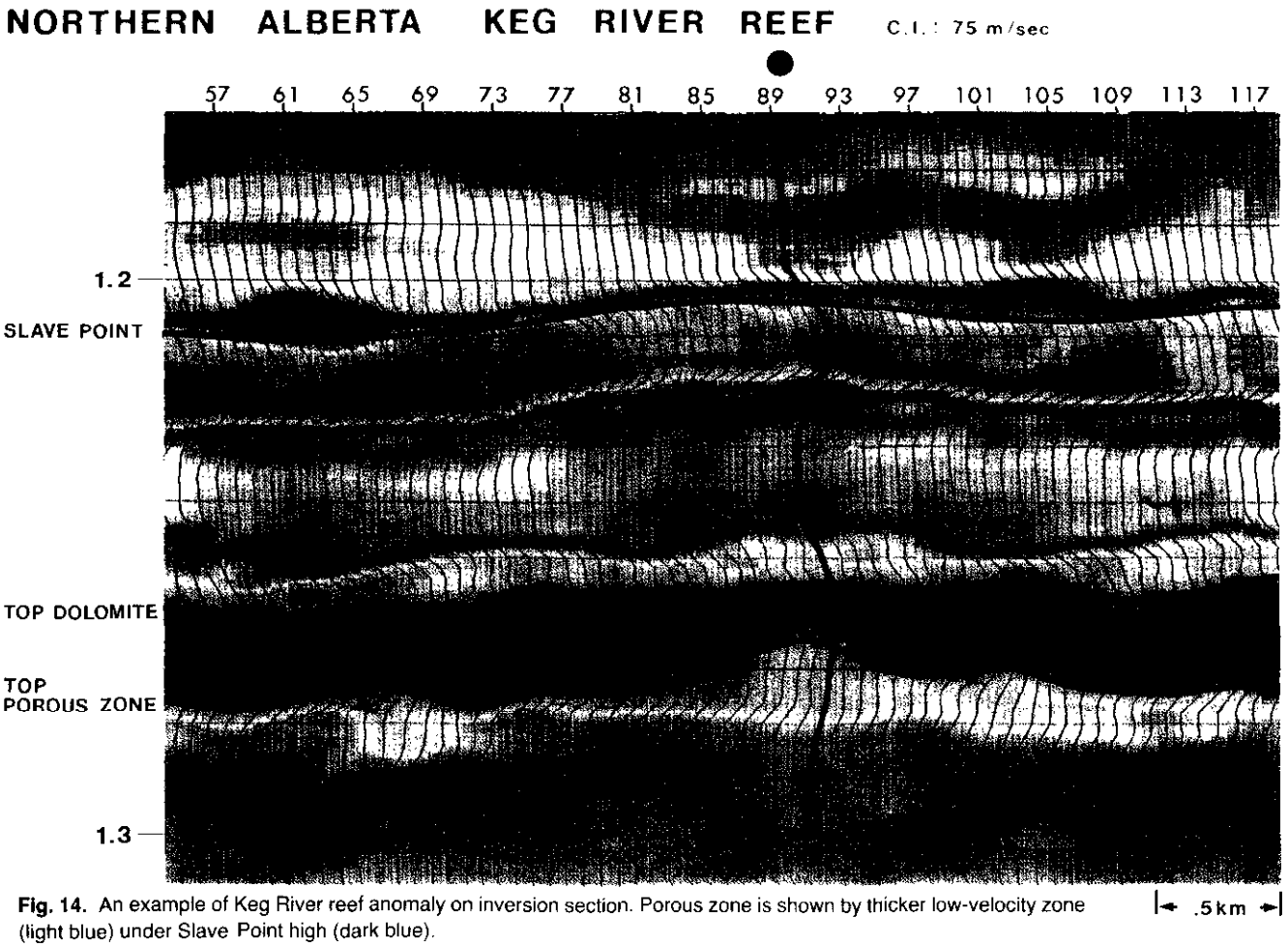

Fig. 14. An example of Keg River reef anomaly on inversion section. Porous zone is shown by thicker low-velocity zone (light blue) under Slave Point high (dark blue).

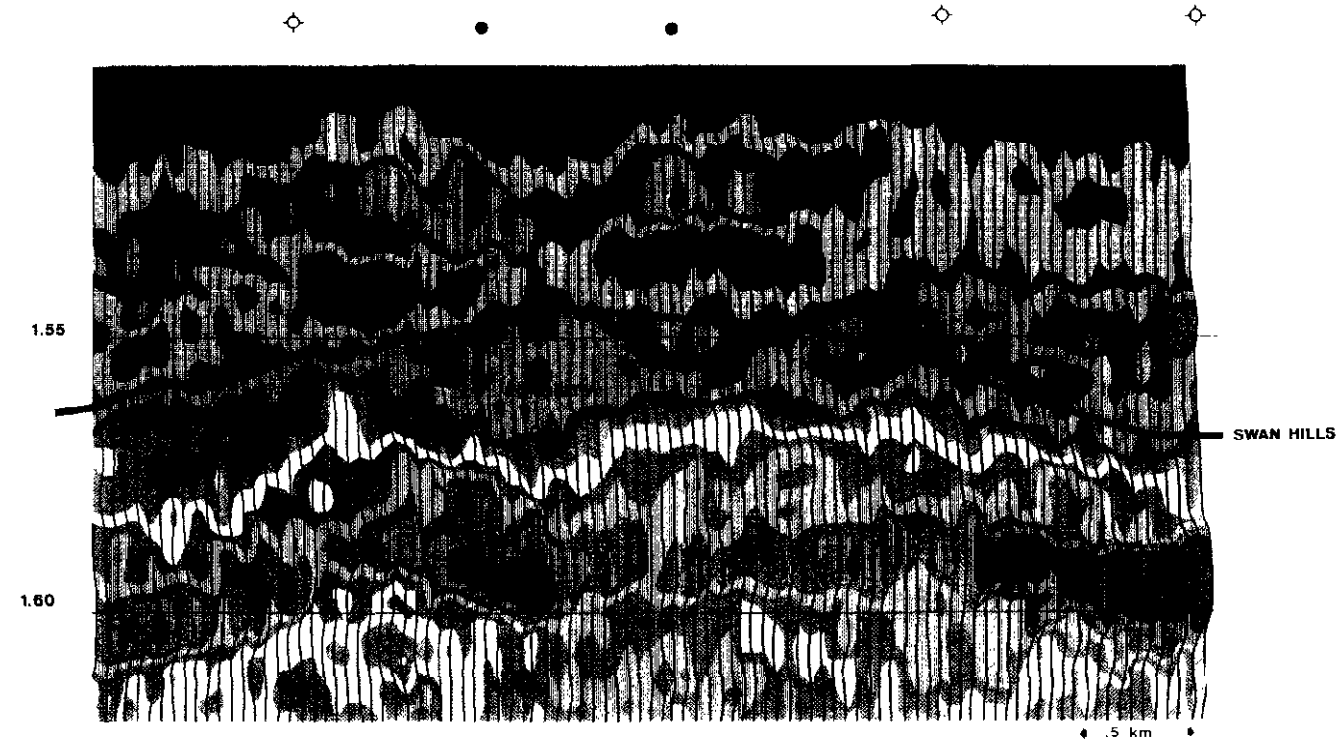

Fig. 15. An example of Swan Hill porosity anomaly on inversion section. The build-up of reef is shown by thickening medium-velocity zone between 1.55 and 1.57 s and porosity by lower-velocity zones indicated by arrows.

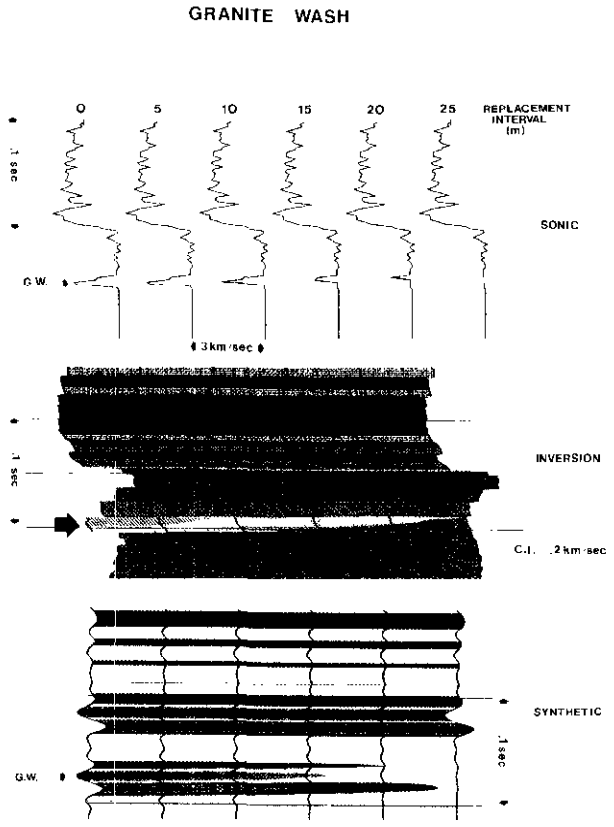

Fig. 16. Granite Wash sand, 25 m thick, thinned from below by one sample (5 m) successively. Inversion predicts velocity change accurately, also indicated by the gradual reduction in Granite Wash reflection event.

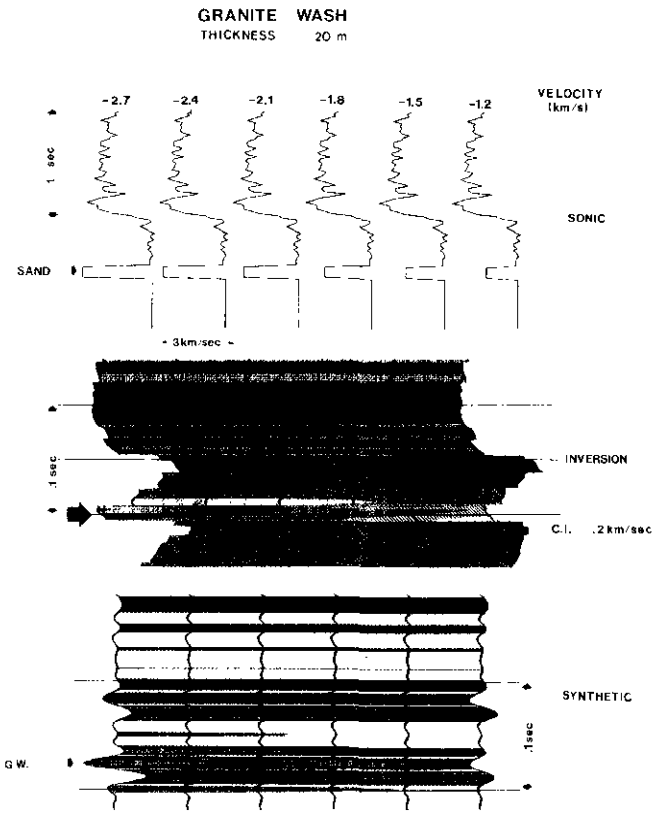

Fig. 17. Granite Wash sand of constant thickness of 20 m and velocity contrast with neighbouring carbonates and granites ranging from 1200 to 2700 m/s.

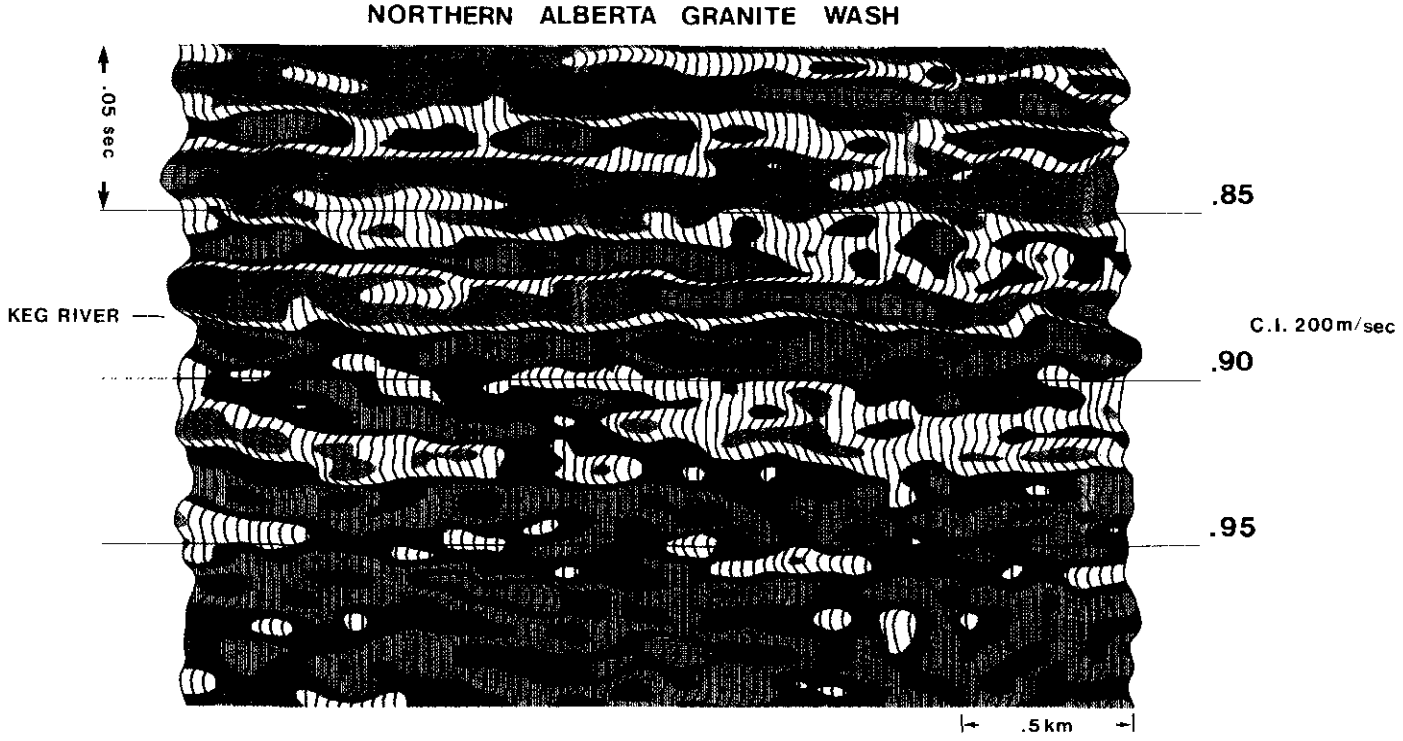

Fig. 18. An example of Granite Wash sand anomaly on inversion section (pale yellow). Zone indicated by the arrow is the likely location of Granite Wash at .90 s.

The sample rate was 2 ms. One sample (5 m) thick sand has a velocity contrast of only 700 m/s but 5 sample (20 m) thick sand has an average velocity contrast of 1200 m/s. Even the thinnest sand is identifiable by a distinct low whose magnitude increases as the sand thickens. Again, the notch is 10 ms wide and reflects a combination of velocity contrast and thickness, rather than accurately representing either or both. This model also shows that any small changes in the Precambrian surface are not likely to be noticed directly, although they may be inferred from the presence of sand.

Figure 17 shows the synthetic where sand thickness is held constant at 20 m and velocity contrast changed from 1.2 to 2.7 km/s. For such contrasts and thickness the inversion traces represent actual velocity contrasts fairly closely. In other words, 20-m-thick sand enveloped by a high-velocity medium is a thick layer for identification purposes.

Figure 18 shows an example of a Granite Wash anomaly on the inversion section from northern Alberta. The arrow indicates thin Granite Wash sands, which appear as a thin, pale yellow strip at .9 s in the middle of the section.

Conclusion

For the four different environments studied here, thin layers cannot be identified specifically but only by general velocity change in the 8-10 ms zone around the anomalous thin zone as compared with the 50-70 ms zone on the stacked section. This is expected to facilitate the isolation of an anomalous zone in actual data, *e.g.* porous sand vs coal bed located at a slightly different level. One can also obtain a qualitative estimate of economic worth from the magnitude of the anomaly but not porosity and thickness separately, unless contrasts are large and/or source is several tens of metres thick.

References

Bower, P. and Boyd, J., 1986, Locating Swan Hills porosity at Judy Creek using seismic inversion: Paper presented at the CSEG National Convention, Calgary, Alberta.

Cooke, D.A. and Schneider, W.A., 1983, Generalized linear inversion of reflection seismic data: Geophysics, v.48, p.665-676.

Delas, G., Beauchomp, J.B., deLombares, G., Fourmann, J.M. and Postic, A., 1970, An example of practical velocity determinations from seismic traces: Paper presented at EAEG, 32nd Meeting in Edinburgh, Scotland.

Gardner, G.H.F., Gardner, L.W. and Gregory, R.A.R., 1974, Formation velocity and density - the diagnostic basics for stratigraphic traps: Geophysics, v.39, p.770-780.

Jain, S., 1985, Some techniques of enhancing seismic reflection data for stratigraphic interpretation: Canadian Society of Exploration Geophysicists Journal, v.21, p.15-29.

_____ and Wren, A.E., 1977, The application of the optimal wavelets in seismic inversion: Canadian Society of Exploration Geophysicists Journal, v.13, p.3-14.

Kuster, G.T. and Toksoz, N., 1974, Velocity and attenuation of seismic waves in two-phase media, Part I: Geophysics, v.39, p.587-606.

Lindseth, R.O., 1979, Synthetic sonic logs, a process for stratigraphic interpretation: Geophysics, v.42, p.3-26.

Oldenburg, D.W., Schurr, T. and Levy, S., 1983, Recovery of acoustic impedance from reflection seismograms: Geophysics, v.48, p.1318-1337.

Telford, W.M., Geldart, L.P., Sheriff, R.E. and Keys, D.A., 1976, Applied Geophysics: Cambridge University Press, p.251-254.

Wren, A.E., 1984, Seismic techniques in Cardium exploration: Canadian Society of Exploration Geophysicists Journal, v.20, p.55-59.